ISBN: 978-3-95450-234-9 ISSN: 2673-5504 doi:10.18429/JACoW-SRF2023-WEPWB128

EXPERIMENTAL STUDY OF MECHANICAL DAMPERS FOR THE FRIB $\beta = 0.041$ QUARTER-WAVE RESONATORS*

J. Brown†, S. H. Kim, T. Xu, W. Hartung, W. Chang
Facility for Rare Isotope Beams (FRIB), East Lansing, MI, USA

Abstract

The 'pendulum' mechanical mode of superconducting quarter-wave resonators (QWRs) can make them vulnerable to microphonics and/or ponderomotive instabilities. Hence QWRs often make use of stiffening or damping. The FRIB QWRs are equipped with Legaro-style frictional dampers inside the inner conductor along with stiffening elements. In cryomodule tests and linac operation, we observed that the damping efficiency is different for a few $\beta = 0.041$ QWRs. This study aimed to experimentally characterize the damping efficacy as a function of the damper mass and surface roughness. We present damping measurements at room temperature at two different masses and surface roughness as well as discuss future studies for damper re-optimization based on this follow-on study.

INTRODUCTION

Quarter-wave resonators present an effective option for acceleration of charged particles or ions. While the two-gap model of the cavity typically limits the operational speeds to low-beta conditions [1], this means the cavity's effective length is shorter. The shorter axial lengths allows more room for other accelerator elements such as magnets and diagnostic tools. QWRs also have a naturally higher shunt impedance which corresponds to higher accelerating efficiency and lower refrigeration power requirements [2].

Mechanical Modes

FRIB utilizes two variations of QWRs, for $\beta = 0.041$ and $\beta = 0.085$, with both operating at 80.5 MHz in linac segment 1. For both of these QWR types, the electric field is heavily concentrated in the short plane near the bottom of the inner conductor. A map of the electric field for the 0.041 QWR can be seen in Fig. 1. External excitations can cause the inner conductor to swing like a pendulum. In a one dimensional case, the inner conductor can be modeled as a oscillating tube with one end fixed and mode resonant frequencies following [3]:

$$\omega_{mech} = \frac{\alpha^2}{L^2}\sqrt{\frac{E_Y I}{\mu}}, \tag{1}$$

where α is a characteristic mode constant, L is the inner conductor length, E_Y is the Young's modulus of the material (niobium for SRF applications), I is the tube's moment of inertia, and μ is the linear mass density of the tube. In typical QWR niobium cavities, the pendulum mode frequencies can range from ~10 Hz to well over 100 Hz, which can be excited by mechanical pumps, thermo-acoustic oscillation in the cryomodule or cryogenic transfer lines. These modes can have high Q_L, and can persist at high amplitudes for long times if excited on resonance [3].

Microphonics

In QWRs, the RLC circuit model frequency is dependent on the charge (and ultimately, the field) distribution on the two gaps. It is this charge and field that make up the capacitance of the cavity. The total capacitance can be expressed as two plate capacitors:

$$C_{cav} = \frac{2\epsilon A}{d}, \tag{2}$$

where A is the cross sectional area in the short plane, ϵ is the permittivity, and d is the accelerating gap length. As the inner conductor swings, d decreases for one gap and increases for the other by some displacement Δx. This changes the capacitance and thus the resonant frequency of the cavity.

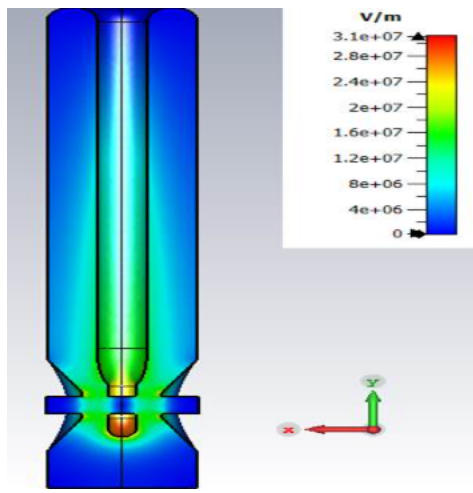

Figure 1: Field map of an FRIB $\beta = 0.041$ QWR from eigenmode simulation in CST Microwave Studio. Field map represents the operational gradient.

Using this lumped circuit model, one can find that $P_f \alpha \Delta f^2$, where P_f is the forward power and Δf is the detuning amplitude. The effective length of the $\beta = 0.041$ cavity is 0.160 m, and thus even small displacements of the inner conductor can lead to large detuning amplitudes due to smaller gap sizes. FRIB keeps the detuning within half of

* Work supported by the US Department of Energy, Office of Science, High Energy Physics under Cooperative Agreement award number DE-SC0018362, used resources of the Facility for Rare Isotope Beams (FRIB), which is a DOE Office of Science User Facility, under Award Number DE-SC0000661, and Michigan State University
† brownjac@frib.msu.edu

ISBN: 978-3-95450-234-9 ISSN: 2673-5504 doi:10.18429/JACoW-SRF2023-WEPWB128

the cavity's cold bandwidth, a point at which the operational P_f approximately doubles.

As it can be seen in Eq. (1), the mechanical mode frequencies depend on the geometry and material of the cavity, things that cannot be changed to preserve operational specifications. In addition to other tuning methods, FRIB uses frictional dampers, the design of which is based on the Legaro-style frictional damper [3], which can be seen in Fig. 2.

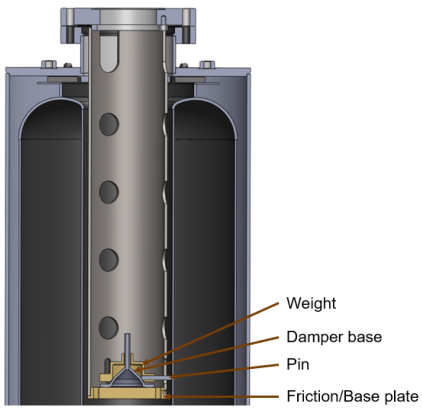

Figure 2: Diagram of FRIB Legaro-style frictional damper.

It has been noted during spare cryomodule tests and linac operation that some of the $\beta = 0.041$ style QWRs experience more detuning than the $\beta = 0.085$ QWRs equipped with the same damper design. This has motivated us to examine the mechanical modes and properties of the dampers of the 0.041 QWRs as possible improvements to linac operation.

METHODS

While the motion of the inner conductor is pendulum in nature, when equipped with the damper and driven with an external force, the system can be modeled as a four spring, two mass system. Figure 3 contains an analytical model of a loaded damper system. In this model m_1 and m_2 are

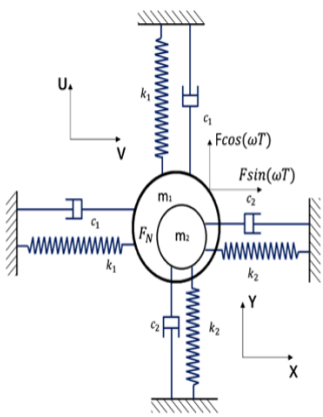

Figure 3: Spring mass system of inner conductor loaded with damper [4].

the effective masses of the inner conductor and damper respectively. The factors k_1 and k_2 are the effective spring constants of their respective masses. Finally, we have the frictional sources c_1 and c_2 corresponding to their respective masses. From this model, we can identify two parameters that we can control easier than others. That is both m_2 and c_2 can be changed simply by increasing/decreasing the weight of the damper or polishing the base plate as to lower the coefficients of friction. Thus we sought to find what changes to the damping profile varying these two parameters caused.

Setup

We created a setup to find and drive mechanical modes and examine the response of the 0.041 QWR cavity. Inspiration for our setup has been drawn from works by INFN-LNL [3] and TRIUMF [4], but has been modified with available equipment. A picture and diagram of our setup can be seen in Fig. 4.

A function generator generates a sine wave of varying amplitude, which is then passed through an audio amplifier, which then shakes the cavity via a speaker latched to the helium jacket at the mechanical resonance frequency. The cavity is driven on its un-perturbed electrical resonance via an RF signal generator. The pick-up power spectrum of the cavity is then analyzed on a real-time signal analyzer (RTSA).

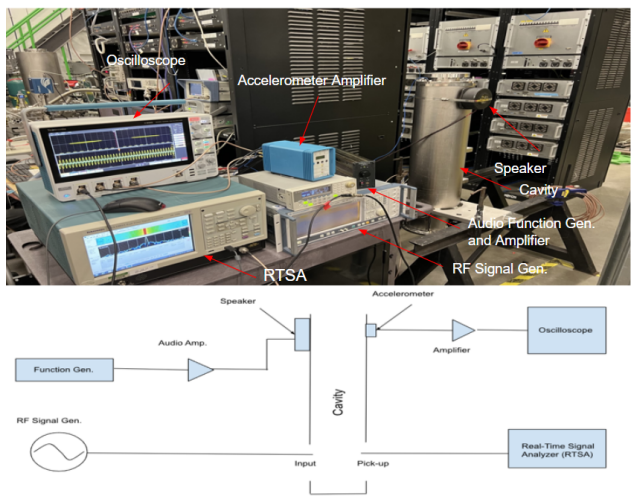

Figure 4: Picture of the setup used to examine damping profiles. Included is an equivalent circuit diagram.

This open-loop setup is equivalent to phase modulation of the cavity pickup signal as the cavity frequency changes with respect to the fixed-frequency input signal. The time varying phase for which can be expressed as Ref. [5]:

$$\phi(t) = A \sum_{n=-\infty}^{\infty} J_n(\Delta\phi) e^{it(\omega_c + n\omega_m)}, \qquad (3)$$

where A is the amplitude coefficient, J_n are Bessel's functions of the first kind, $\Delta\phi$ is the phase difference between the RF clock and cavity, and ω_c and ω_m are the carrier and modulating frequencies respectively. From Eq. (3), it can be

ISBN: 978-3-95450-234-9 ISSN: 2673-5504 doi:10.18429/JACoW-SRF2023-WEPWB128

shown that the side-band power in units of decibels relative to the carrier (dBc) can be expressed as:

$$P_{sb}[dBc] = 10\log_{10}\frac{J_1^2(\Delta\phi)}{J_0^2(\Delta\phi)}. \quad (4)$$

The side-band power can be measured from the RTSA and used to calculate $\Delta\phi$. Once $\Delta\phi$ is known, the detuning amplitude Δf can be calculated via the following expression,

$$\Delta f = \frac{BW}{2}\tan(\Delta\phi), \quad (5)$$

where BW is the cavities unperturbed bandwidth. At room temperature, we expect that the $BW \gg \Delta f$, thus first order approximations can be used for Bessel's functions since $\Delta\phi \ll 1$.

Accelerometers were attached to the top of the helium jacket and the responding voltage responses are passed through a x10 amplifier and displayed on an oscilloscope. The amplitudes from the oscilloscope are then captured via a LabVIEW program. The voltage amplitudes are proportional to the displacement amplitudes of the top of the cavity. For small displacements of the inner conductor ($\Delta x \ll d$), we should find that $\Delta f \propto \Delta x^2$. Thus plotting detuning amplitudes against displacment amplitudes should yield a parabolic curve for small displacement relative to the gap length.

The function generator amplitude was varied from 0 to 1000 mV while the RTSA recorded the pickup signal for a minute. The accelerometer responses were recorded over two minutes as the accelerometers are quite sensitive to noise and thus a longer averaging time was required. This process was utilized for four cases:

- No damper installed.
- Un-modified damper installed in the cavity.
- Damper with an extra ~ 10% mass added.
- Damper with original mass and polished base plate.

RESULTS

Expressing Bessel's functions to first order, we can utilize $J_0 \approx 1$ and $J_1 \approx \frac{\Delta\phi}{2}$. Using logarithm rules and Eq. (4), we can rewrite Eq. (5) as:

$$\Delta f = \frac{BW}{2}\tan(2\times 10^{P_{sb}/20}). \quad (6)$$

Thus we can calculate the detuning amplitude from our time data via a Python script. As the audio amplifier gain is unknown to us, detuning amplitudes were plotted with the corresponding measured displacement amplitudes. From roughness measurements, it was found that that pre-polishing, the roughness average (Ra) was at most 3.05 µm. Post-polishing, the Ra was measured to be 0.203 µm.

The resulting curves for a $f_{m1} = 32.775$ Hz mode and its shifts can be seen in Fig. 5. Results for our phase excursion $\Delta\phi$ calculation at first order show little difference to values calculated with J_0 and J_1 written out to 50 terms via Python. For comparison, a plot of the detuning amplitudes plotted against the function generator voltage can be seen in Fig. 6.

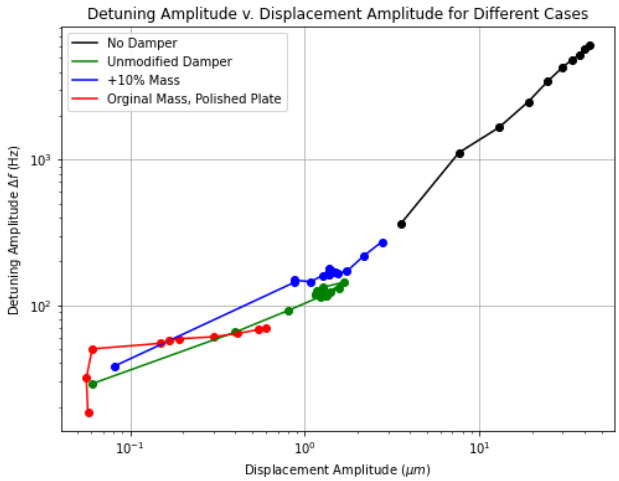

Figure 5: Plot of detuning amplitude versus displacement amplitude for the first high-Q mode over the four cases of testing.

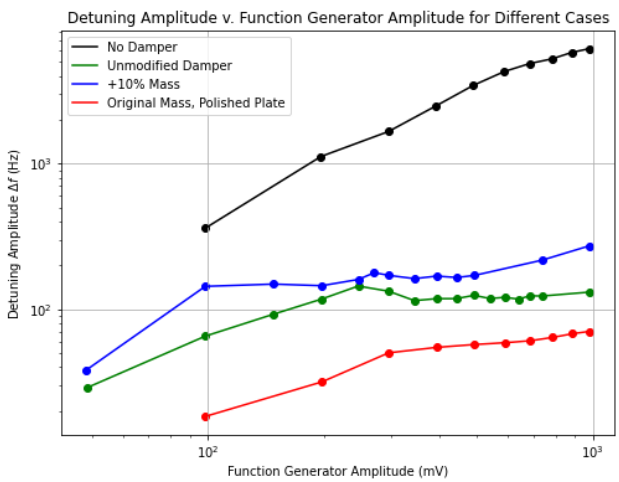

Figure 6: Plot of detuning amplitude versus function generator amplitude for the first high-Q mode over the four cases of testing.

No data was collected for the f_{m2} =33.085 Hz mode save for the no damper and polished plate case. The results for both cases can be seen in Fig. 7.

Decay measurements were utilized to measure the Q_L factors of the modes with no damper and at points of overall decreased detuning amplitude. The resulting Q_L's at the mode frequencies can be seen in Table 1.

CONCLUSIONS AND OUTLOOK

We find that polishing the base plate is an effective means for reducing detuning amplitudes, as can be seen in Figs.

ISBN: 978-3-95450-234-9 ISSN: 2673-5504 doi:10.18429/JACoW-SRF2023-WEPWB128

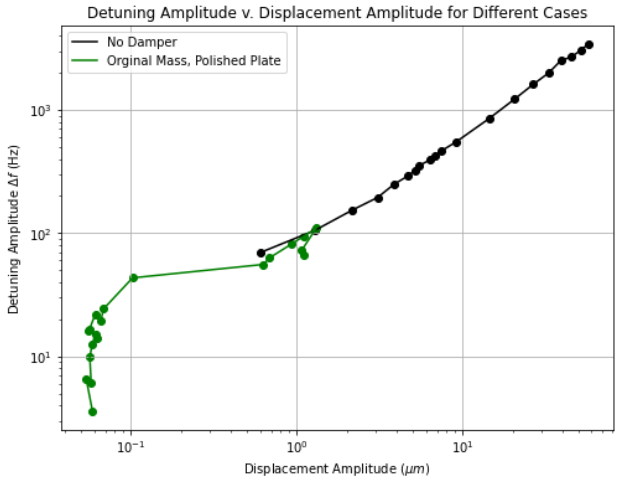

Figure 7: Plot of detuning amplitude versus displacement amplitude for the second high-Q mode over two cases of testing.

Table 1: Table of mode frequencies and Q_Ls. The mid-line separates the two modes.

Frequency [Hz]	Configuration	Q_L
32.775	No Damper	2249.86
34.805	Linac Damper	1303.90
34.805	Polished Plate	90.0803
33.085	No Damper	965.1590
35.785	Polished Plate	56.6660

5, 6, and 7. Figures 5 and 7 shows that for larger regions of measured displacement the detuning increases at a much slower rate in the polished plate case. We find that the once the damper activates, the detuning increases slowly, then approaches a linear trend at higher function generator amplitude for some cases. The no damper case shows a solid linear trend, suggesting displacements of the inner conductor comparable to the gap length.

As can be seen in Fig. 6, we see that our initial added-mass case shows an increase detuning, which agrees with the study results from TRIUMF [4]. Even with the plate being polished, the damping profile does not yet meet the ideal damping goal of less than half of $\beta = 0.041$ loaded bandwidth (~20 Hz). Thus this work will serve as preliminary guide for future studies, with an overall goal of finding optimized values for the damper mass and coefficient of friction.

For all future measurements, the function generator amplitude will be swept out to higher set-points to better see damping trends. Finer steps will also be used to better understand the behavior of the damper at different damping regions. The measurements of the unmodified damper will be retaken with a spare plate and data for $f_{m'}$ will be collected. Figure 7 shows interesting behavior in the polished-plate case in where after 800 mV both the detuning and displacement amplitudes drop. We believe this shows the regime in which the friction between the damper and the base plate becomes kinetic. Figure 6 shows a similar drop in the unmodified damper and added mass case, but at a much earlier at 250 mV. The polished-plate case in Fig. 6 shows no such transition up to 1000 mV. Thus we will strive to better understand this transition in future studies.

REFERENCES

[1] T. Wangler, *RF Linear Accelerators*, Wiley-VCH, Weinheim, 2008, p. 121.

[2] I. Ben-Zvi and J.M. Brennan, *The Quarter Wave Resonator as a Superconducting Linac Element*, *Nucl. Instrum. Methods Phys. Res.*, vol. 212, pp. 73–79, 1983. doi:10.1016/0167-5087(83)90678-6

[3] A. Facco, "Mechanical Mode Damping in Superconducting Low β Resonators", in *Proc. SRF'97*, Padova, Italy, Oct. 1997, paper SRF97C31, pp. 685–694.

[4] L. Yang, V. Zvyaginstev, R.E. Laxdal, and B. Waraich, *Damping of Vibrations in Superconducting Quarter Wave Resonators*, *Phys. Rev. Accel. Beams*, vol. 22, 2019. doi:10.1103/PhysRevAccelBeams.22.030103

[5] F. Stocklin, *Relative Sideband Amplitude vs. Modulation Index for Common Functions Using Frequency and Phase Modulation*, NASA, USA, NASA-TM-X-70517, 1973.